


Research Article

DOA Estimation Method Based on Multi-Layer Neural Networks

Ruiyan Cai¹, Yuxuan Lei¹, Quan Tian^{1*}, Songlin Guo²

¹School of Artificial Intelligence, Taizhou University, Taizhou, 318000, China

²State Grid Shanghai Electric Power Engineering Construction Consulting Company, Shanghai, 200120, China
E-mail: tianquan10@163.com

Received: 26 July 2025; **Revised:** 27 August 2025; **Accepted:** 2 September 2025

Abstract: As a subject of extensive research in numerous scientific and engineering disciplines, the Direction of Arrival (DOA) estimation leads to the creation of numerous specialized algorithms. As deep learning continues to evolve, it has progressively reshaped the field of DOA estimation, bringing forth new opportunities. Traditional DOA estimation algorithms typically require manual feature selection and model design; however, deep learning inherently extracts features and patterns from data autonomously, thus providing more accurate and robust DOA estimation. Within deep learning architectures, the MultGRU algorithm is proposed as a novel solution for DOA estimation. This algorithm employs Gated Recurrent Unit (GRU) to attain accurate DOA estimation. The MultGRU adopts a two-level architecture: The first-level GRU network performs coarse localization by mapping the target DOA to large angular intervals (5° each within $0^\circ \sim 90^\circ$) using array covariance matrix features. The second-level employs some parallel subGRU networks with 5° overlap between adjacent subGRUs to subdivide the coarse intervals into 0.1° fine-grained intervals. A probability-weighted correction mechanism is integrated to optimize estimates by fusing predictions from adjacent intervals to effectively reduce estimation errors. Experiments are conducted to compare the MultGRU with other DOA estimation algorithms under different numbers of snapshots and sensors, varying Signal-to-Noise Ratios (SNR), and in dual-source scenarios. The DOA estimation accuracy of the MultGRU is improved by more than 29% overall, and its computational efficiency is higher than theirs.

Keywords: low-altitude radio, neural networks, Direction of Arrival (DOA) estimation, Gated Recurrent Unit (GRU)

MSC: 68T05, 94A13

1. Introduction

Direction of Arrival (DOA) estimation is, in essence, defined as the process of ascertaining the angular location corresponding to the signal's origin [1]. The significance of DOA estimation lies in its ability to provide spatial information about signal sources, enabling efficient processing and optimization of array systems. This allows for improved signal separation, identifying interference sources, noise reduction, and enhanced target detection and tracking [2, 3]. By accurately estimating the DOA, the performance of beamforming algorithms can also be enhanced, which can suppress interference and focus the array response on the desired source.

In recent years, to cope with various signal environments, many new DOA estimation algorithms have been developed. For example, researchers proposed an algorithm to improve DOA estimation by reconstructing noise [4].

Initially, a coarse estimation of the noise component is obtained. Then, a new cumulative sum is created to reconstruct the noise component accurately. Finally, by utilizing the denoised data, DOA estimation can be obtained. Manifold ambiguity is an inherent defect of the unfolded coprime array, and to solve this problem, the Support Vector Regression (SVR) method was proposed. For the received signals, the SVR uses the eigenvectors to estimate DOAs. The SVR boasts both high DOA estimation accuracy and low computational complexity [5]. To address the reduced DOA estimation capability of automotive radar under low Signal-to-Noise Ratio (SNR) due to mutual interference, a novel algorithm was proposed by Integrating Multiple Signal Classification (MUSIC) [6] and Empirical Mode Decomposition (EMD) [7]. A real-valued Toeplitz matrix algorithm based on an optimized coprime array was proposed to carry out DOA estimation [8]. Based on real-valued Sparse Bayesian Learning (SBL), [9] proposed a low-complexity algorithm with an innovative three-stage design to improve the real-time capability of DOA estimation: firstly, real-valued transformation of the covariance matrix is adopted to reduce the computational complexity; secondly, a novel fixed-point iteration method based on the probability distribution of noise variance is proposed; finally, a dynamic grid partitioning strategy is employed to improve the estimation accuracy. Furthermore, simulations demonstrate that the algorithm significantly enhances the computational speed while maintaining the estimation accuracy. A DOA estimation method for non-circular signals based on nested arrays and off-grid sparse Bayesian learning is proposed [10]. By jointly expanding the aperture with virtual difference/sum co-arrays, the noise variance is incorporated into the signal iteration to optimize grid points, which significantly improves the estimation accuracy and degrees of freedom. Under impulsive noise environments, by leveraging the Fast Iterative Shrinkage-Thresholding Algorithm (FISTA), a novel method was proposed to enhance the DOA estimation accuracy [11]. By combining Gaussian noise and outliers to model impulsive noise, the sparse characteristics of the outlier matrix are made use of to accomplish snapshot-wise optimization. Combined with an alternating iteration algorithm to address the off-grid issue, this method significantly improves resolution and estimation accuracy under strong impulsive noise environments.

In the domain of array signal processing, deep learning serves as a vital component, underpinning the efficiency and accuracy of key tasks [12, 13]. Deep learning can extract complex and non-linear features from high-dimensional array output signals in various applications; so, it enables us to overcome challenges such as signal interference, noise, and reverberation, enabling accurate localization and tracking for the source. Traditional DOA estimation algorithms rely on manually selected features and assumptions of signal models, which can be limited in capturing the effective signal information in real-world scenarios. Deep learning-based algorithms can automatically learn potential features directly from array output signals, leading to improved accuracy and robustness in DOA estimation. Furthermore, an end-to-end learning mechanism can be realized through deep learning, which enables the integration of different stages of DOA estimation into a single network. This streamlines the system structure while simultaneously improving the overall performance through the joint optimization of different components.

To address the DOA estimation task for multiple narrowband sources, a novel end-to-end deep learning algorithm has been put forward [14]. This algorithm can provide reliable DOA estimation in environments with array mismatch, low SNR, and few snapshots. Through the integration of massive Multiple-Input Multiple-Output (MIMO) technology, [15] proposed a new Deep Neural Network (DNN) framework. The training process of this DNN framework starts with offline learning, where simulated data under different channel conditions is trained; afterwards, online learning is applied to obtain output data that corresponds to the input data. On this basis, two DOA estimation methods are derived. On the premise of an unknown number of multipaths in the signal, by introducing deep learning into the millimeter-Wave (mmWave) massive MIMO system, a new DOA estimation method was proposed [16]. To address DOA estimation for uniform linear arrays under low SNR, an improved method that leverages star-transformer was proposed [17]. By formulating DOA estimation as a multi-label classification task, this method decomposes the covariance matrix into three components: phase, imaginary, and real components. This method shows excellent robustness and efficiency in various conditions like different SNRs, snapshots, and signal mismatches. By using low-resolution Analog-to-Digital Convertors (ADCs), transMUSIC, which serves as a transformer-assisted subspace method for DOA estimation, was proposed [18]. It processes snapshots in parallel to capture global correlations, enabling gridless estimation and source number determination, showing superiority even with one-bit data. Zhao et al. [19] explored Bidirectional Encoder Representation from Transformer (BERT) with a physics-based loss for sea surface DOA estimation, outperforming Long

Short-Term Memory (LSTM) and BERT with Mean Square Error (MSE), especially under high noise levels and large datasets, and showing adaptability to wind scales and superiority in co-polar and full-bistatic modes.

The low-altitude economy, serving as an emerging strategic field, comprises application scenarios like drone logistics and urban air mobility.

The safe operation and management of low-altitude economy rely on the precise monitoring and positioning of Unmanned Aerial Vehicles (UAVs).

Since traditional DOA estimation algorithms have drawbacks-especially when focusing on achieving high-precision positioning of low-altitude UAVs and when there is no prior knowledge regarding array geometry configurations, signals, and noises-this paper proposes a deep learning-based algorithm, termed MultGRU, that fuses spatio-temporal features to analyze signal patterns.

The algorithm can be embedded in low-altitude monitoring radars and other monitoring facilities to provide high-precision DOA estimation for scenarios such as air traffic control and unauthorized flight tracking.

It helps build a digital low-altitude management system and breaks through the performance bottlenecks of traditional algorithms.

The main research works are listed as follows:

- In the first-level of the MultGRU, a new Gated Recurrent Unit (GRU) network is designed to implement coarse interval classification for DOA estimation, which maps the DOA of the target source to several connected angular intervals with large ranges.

- In the second-level of the MultGRU, the three consecutive classification intervals of the first-level are merged into a single large interval. Subsequently, multiple subGRU networks are designed, with each subGRU network covering one large interval. This large interval is then further subdivided to achieve high-precision DOA estimation.

For DOA estimation, MultGRU demonstrates significant advantages over commonly used networks like Convolutional Neural Network (CNN), LSTM, and Recurrent Neural Network (RNN). In terms of handling overlapping sources, CNN is limited by its fixed receptive field and dependence on spatial topology, making it difficult to resolve subtle angular differences. RNN and LSTM, which focus on temporal modeling, introduce redundant computations for static array signals and are prone to feature confusion. In contrast, MultGRU effectively improves the resolution of overlapping sources through a two-level hierarchical parsing mechanism, combined with multiple parallel sub-networks to capture multi-peak features, followed by probability-weighted fusion.

Furthermore, regarding adaptability to changes in array geometry, CNN, RNN, and LSTM are highly affected by input dimensions and structures, resulting in poor generalization. MultGRU, however, learns the statistical properties of covariance matrices. Its two-level architecture reduces dependence on specific array topologies, and probability fusion enhances stability across geometric scenarios, making it more suitable for complex DOA estimation scenarios.

Throughout this paper, the following notations apply. Superscripts ‘T’ and ‘H’ represent the transpose operations and the conjugate transpose of matrices, respectively.

2. Problem formulation

2.1 Uniform circular array signal model

Considering a Uniform Circular Array (UCA) with a radius R comprising N sensors [20], the position of the n -th sensor can be determined as follows:

$$\mathbf{r}_n = R \left[\cos \left(\frac{2\pi(n-1)}{N} \right), \sin \left(\frac{2\pi(n-1)}{N} \right) \right]^T, \quad n = 1, 2, \dots, N. \quad (1)$$

The steering vector of the UCA is an essential component that encapsulates the phase shifts experienced by the signal as it impinges on the UCA from a specific direction. Assuming a signal arrives at the UCA from azimuth θ and elevation ϕ , $\mathbf{a}(\theta, \phi)$ denotes the steering vector that can be described as follows:

$$\mathbf{a}(\theta, \phi) = \left[e^{jkR \sin(\phi) \cos(\theta - \theta_0)}, e^{jkR \sin(\phi) \cos(\theta - \theta_1)}, \dots, e^{jkR \sin(\phi) \cos(\theta - \theta_{N-1})} \right]^T \quad (2)$$

In Equation (2), $k = 2\pi/\lambda$ represents the wavenumber and the wavelength is λ . $\theta_0, \theta_1, \dots, \theta_{N-1}$ represent the phase offset angles of each sensor relative to the reference sensor.

In vector form, the array output signals can be written as follows:

$$\mathbf{x}(t) = \sum_{m=1}^M s_m(t) \mathbf{a}(\theta_m, \phi_m) + \mathbf{n}(t) \quad (3)$$

In Equation (3), $s_m(t)$ is the complex amplitude corresponding to the m -th source, $\mathbf{a}(\theta_m, \phi_m)$ is the steering vector for the m -th source, and $\mathbf{n}(t)$ is the noise vector.

2.2 The MUSIC algorithm

Given a sufficient number of snapshots T , the sample covariance matrix \mathbf{R}_x can be approximated as follows:

$$\mathbf{R}_x = \frac{1}{T} \sum_{t=1}^T \mathbf{x}(t) \mathbf{x}^H(t) \quad (4)$$

Further, after the covariance matrix \mathbf{R}_x is performed Singular Value Decomposition (SVD), we arrive at:

$$\mathbf{R}_x = \mathbf{U}_s \mathbf{\Lambda}_s \mathbf{U}_s^H + \mathbf{U}_n \mathbf{\Lambda}_n \mathbf{U}_n^H \quad (5)$$

Equation (5) defines \mathbf{U}_s and \mathbf{U}_n as the eigenvectors belonging to the signal and noise subspaces, with $\mathbf{\Lambda}_s$ and $\mathbf{\Lambda}_n$ serving as the associated eigenvalue matrices.

The formulation of the pseudospectrum is given by:

$$P(\theta, \phi) = \frac{1}{\mathbf{a}^H(\theta, \phi) \mathbf{U}_n \mathbf{U}_n^H \mathbf{a}(\theta, \phi)} \quad (6)$$

Then, by performing a spectral peak search, the angle (θ, ϕ) of the source can be determined. This corresponds to the MUSIC algorithm.

3. The deep learning-based DOA estimation

For DOA estimation, deep learning exhibits several advantages: (1) High accuracy: Deep learning networks are capable of learning feature representations from large amounts of data, possessing powerful expressive capabilities to capture complex signal features through multi-layer nonlinear transformations. (2) Strong adaptability: Deep learning networks can be trained and adjusted according to different environments and scenarios, making them more reliable and robust in practical applications. (3) End-to-end learning: Deep learning networks are capable of directly extracting DOA estimates from raw sensor data through an end-to-end learning approach, simplifying the cumbersome feature extraction

and processing procedures in traditional methods. (4) Scalability: Deep learning networks can be expanded and optimized by increasing the number of network layers, adjusting parameters, and gradually improving accuracy and performance. In general, deep learning networks can provide powerful tools and methods for achieving accurate target localization and separation [21, 22].

As a key component within deep learning networks, the RNN is highly successful in modeling sequential data, but it also faces the problem of vanishing gradients. The GRU is a variation of the RNN that incorporates gate mechanisms to manage information flow and update memory [23]. Therefore, based on the GRU, a new Multiple GRU (MultGRU) algorithm is proposed to achieve high-precision DOA estimation. The structure of the GRU cell is as illustrated in Figure 1.

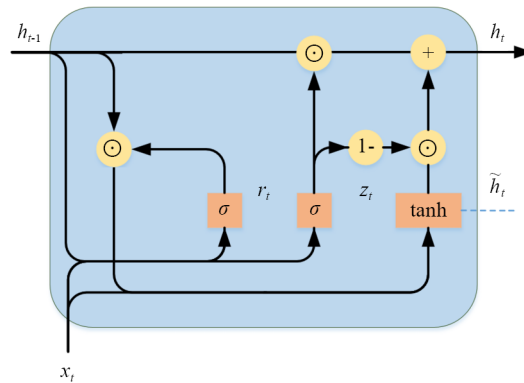


Figure 1. The structure of the GRU cell

3.1 Data preprocessing

DOA estimation based on deep learning networks essentially aims to achieve a specific mapping: converting array output signals into the DOA of the source. Take into account a UCA with N sensors, according to Equation (4), the covariance matrix $\mathbf{R}_x \in \mathbb{C}^{N \times N}$ can be obtained. Since the input of the GRU must be a real-valued sequence, \mathbf{R}_x must be converted into a real-valued serialized form.

\mathbf{R}_x will be transformed into the following form:

$$\mathbf{R}'_x = [\text{real}(\mathbf{R}_x), \text{imag}(\mathbf{R}_x)] \quad (7)$$

In Equation (7), $\text{imag}(\cdot)$ and $\text{real}(\cdot)$ represent the imaginary and real components in that order. It can be found that the dimensions of \mathbf{R}'_x are $N \times 2N$.

The serialization of \mathbf{R}'_x can be done according to the following steps. By defining $\mathbf{R}'_x(i, :)$ as the i -th row of \mathbf{R}'_x , $i = 1, 2, \dots, N$, we can obtain:

$$\mathbf{R}' = [\mathbf{R}'_x(1, :), \mathbf{R}'_x(2, :), \dots, \mathbf{R}'_x(N, :)] \quad (8)$$

By normalizing \mathbf{R}' , we can obtain:

$$\mathbf{R}'' = \frac{\mathbf{R}'}{\|\mathbf{R}'\|_2} \quad (9)$$

To handle the situation where the UCA contains different numbers of sensors, we need to expand Equation (9). Assume that the UCA contains a maximum of N_{\max} sensors, that is, $N_{\max} \geq N$. Then, \mathbf{R} will be rewritten as follows:

$$\mathbf{R} = [\mathbf{R}'', \underbrace{0, \dots, 0}_{2(N_{\max}^2 - N^2)}] \quad (10)$$

If the true DOA corresponding to \mathbf{R} is defined as P , then we establish the pairs $\{\mathbf{R}_u, P_u\}_{u=1}^U$, which can be used as the dataset for training and validating the MultGRU, and this dataset consists of U pairs.

3.2 The MultGRU algorithm

In a multi-hierarchical framework, the GRU resists overfitting and enables efficient parallel training. Experiments also show it outperforms the LSTM in similar tasks, with faster inference and a smaller model size, making it ideal for short-dependence signal classification.

Traditional super-resolution subspace-based DOA estimation algorithms, like the MUSIC, achieve DOA estimation via spectral peak search, the minimum interval of spectral peak search determines the DOA estimation accuracy. Similarly, deep learning-based DOA estimation algorithms are also considered to be classification problems; therefore, the minimum interval of the angle classification also determines the DOA estimation accuracy.

Assuming the angle range is $[0^\circ, 90^\circ]$, if the GRU is used to perform DOA estimation with a small interval set to 0.1° , experiments have shown that the accuracy of training and validation is only close to 50%, which cannot achieve high-precision DOA estimation. Therefore, by using multiple GRUs, the MultGRU algorithm is proposed. The structure of the MultGRU can be found in Figure 2.

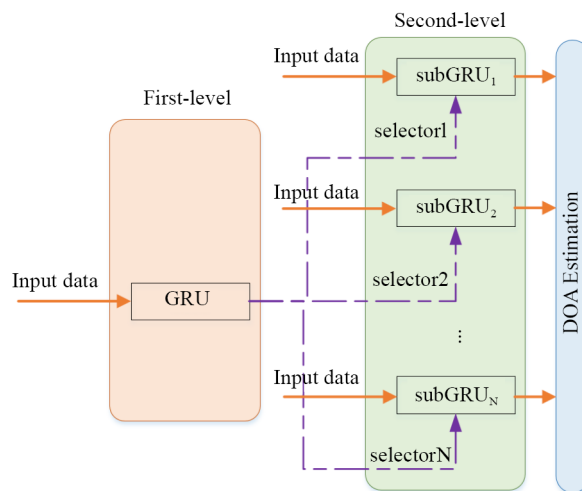


Figure 2. The structure of the MultGRU network

For the MultGRU, the input consists of two parts, one is the real-valued sequence obtained by preprocessing the array output signals, and the other is the incident angle corresponding to each real-valued sequence. It should be noted that the incident angle here is divided into larger intervals: $[0^\circ : 5^\circ : 90^\circ]$. That is, if the incident angle is defined as θ_u , for the first-level, its corresponding training label P_u can be expressed as follows:

$$P_u = \lfloor \theta_u / 5 \rfloor + 1 \quad (11)$$

In Equation (11), $\lfloor \cdot \rfloor$ represents rounding.

The first-level, which can be found in Figure 3, includes six layers: a sequence input layer, two GRU layers, a fully connected layer, a softmax layer, and a classification layer. The number of hidden units of the two GRU layers is 60 and 20, respectively.

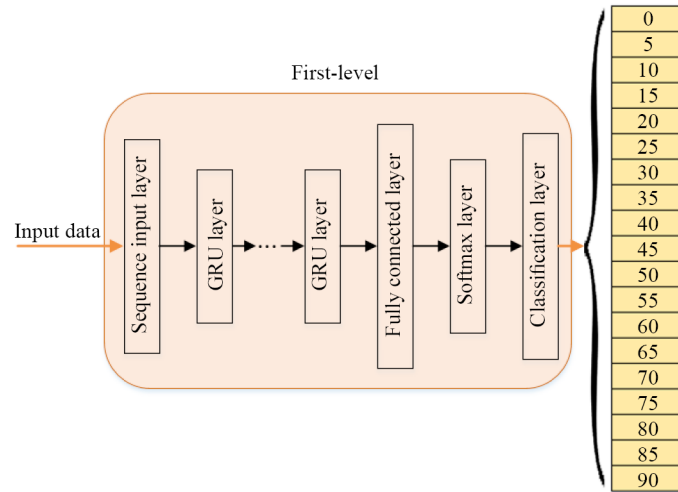


Figure 3. The first-level of the MultGRU

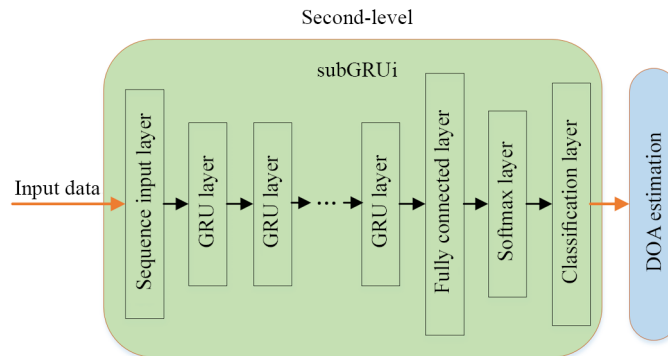


Figure 4. The second-level of the MultGRU

Figure 4 depicts the second-level structure. It can be found that the second-level includes multiple subGRU networks, called the subGRU_i ($i = 1, 2, \dots, 9$). Each subGRU includes seven layers: a sequence input layer, three GRU layers, a fully connected layer, a softmax layer, and a classification layer. The number of hidden units of the three GRU layers is 60, 30, and 20, respectively.

Similar to the first-level, during subGRU training, the input data is a real-valued sequence formed by preprocessed array output signals, but the labels corresponding to the real-valued sequences are different. To obtain high-precision DOA estimation, each subGRU divides the 15° range into segments with a 0.1° interval. Figure 5 presents the criterion for selecting which subGRU to be used in the second-level.

Sub network	Angle interval
subGRU ₁	0° ~ 14°
subGRU ₂	10° ~ 24°
subGRU ₃	20° ~ 34°
subGRU ₄	30° ~ 44°
subGRU ₅	40° ~ 54°
subGRU ₆	50° ~ 64°
subGRU ₇	60° ~ 74°
subGRU ₈	70° ~ 84°
subGRU ₉	80° ~ 90°

Figure 5. Selection criterion for the subGRU

Consider the output of the second-level, assuming the estimated DOA is θ_e and its corresponding probability is p . With the aim of further elevating the accuracy of DOA estimation, assuming the prediction probability of $(\theta_e - 0.1^\circ)$ is p_1 and the probability of $(\theta_e + 0.1^\circ)$ is p_2 , the final result of the DOA estimation can be calculated as follows:

$$\theta_{\text{DOA}} = \theta_e \cdot p + (\theta_e - 0.1^\circ) \cdot p_1 + (\theta_e + 0.1^\circ) \cdot p_2 \quad (12)$$

For the case where the incident source angle lies in the overlapping region of two subGRUs, the DOAs, which are estimated by Eq. (12) in the two subGRUs, are calculated, and their mean is taken as the end DOA estimation result.

4. Simulations

This section involves conducting simulation experiments across diverse scenarios and analyzing the results. To assess the performance of the MultGRU, it is compared against existing DOA estimation algorithms, namely the MUSIC, the Covariance Matrix-based Multi-Layer Perceptron (CM-MLP) [24], the Covariance Matrix-based CNN (CM-CNN) [25], and the Estimation of Signal Parameters via Rotational Invariance Techniques (ESPRIT) [26], in which the ESPRIT and the MUSIC are model-based algorithms and the CM-MLP and the CM-CNN are deep learning-based algorithms.

As an essential theoretical tool, the Cramer-Rao Bound (CRB) [27] functions as the theoretical lower bound pertaining to the variance of estimation. It can evaluate algorithm performance, guide system parameter optimization, determine estimation feasibility, and provide objectives for new algorithm design. Thus, the CRB is introduced into experiments to assess the performance of the MultGRU.

4.1 Simulation setup and training settings

Under the premise that the sensor spacing equals half a wavelength, we assume that a unit-power Quadrature Phase-Shift Keying (QPSK) signal impinges on a UCA consisting of 8 sensors.

The Root Mean Square Error (RMSE) helps assess the accuracy of a predictive model [28, 29]. Therefore, the RMSE, which can be expressed as follows, serves to measure the DOA estimation accuracy of various algorithms:

$$\text{RMSE} = \sqrt{\frac{1}{N} \sum_{n=1}^N (\hat{\theta}(n) - \theta_r)^2} \quad (13)$$

In Equation (13), N represents the total DOA estimation runs, θ_r denotes the true DOA, and $\hat{\theta}(n)$ is the estimate of θ_r from the n -th DOA estimation.

For training and validating the MultGRU, four variable parameters come into consideration. These include the SNR, the incident angle θ , the number of snapshots M , and the number of sensors N . The parameter setups are displayed in Table 1.

Table 1. The parameter settings for the MultGRU

Parameter	Interval
SNR	[0 dB : 1 dB : 15 dB]
θ	[0° : 0.1° : 90°]
M	[100 : 100 : 1,000]
N	[6 : 1 : 12]

For each combination of the four parameters, 500 sampling data points are produced. These data, along with their corresponding DOAs, constitute a dataset. We randomly allocate 80% of this dataset to serve as the training set, leaving the remaining 20% as the validation set. Key hyperparameters are listed in Table 2.

Table 2. The hyperparameters of the MultGRU

Parameter	GRU	subGRU _{<i>i</i>}
Learning rate	0.001	0.001
Mini batch size	32	64
Epochs	200	300
Optimizer	Adam	Adam
Regularization parameter	0.0001	0.0001

4.2 Performance under different SNRs

In this section, the SNR is adjusted to fall in the range between 0 dB and 15 dB. The number of snapshots is set to 300.

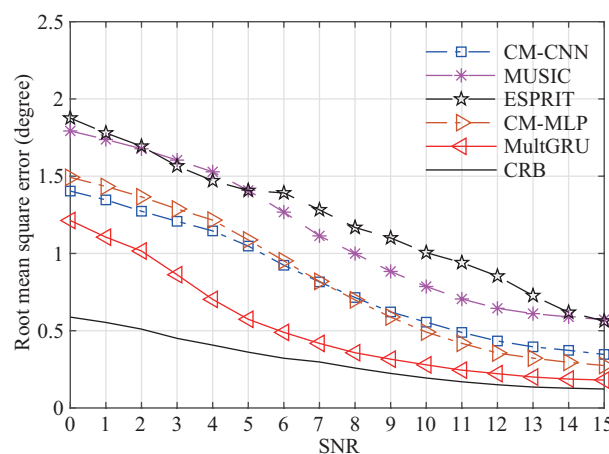


Figure 6. Performance comparison of various algorithms as a function of the SNR

Observations reveal that as SNR increases in Figure 6, all algorithms exhibit a consistent decline in their RMSE curves. For a given SNR, the RMSEs of the ESPRIT and the MUSIC are relatively larger compared to those of other algorithms. Specifically, when examining deep learning-based CM-CNN and CM-MLP, their RMSEs under the same SNR condition are notably lower than those of the MUSIC and the ESPRIT, suggesting that these two algorithms demonstrate better DOA estimation accuracy. For the MultGRU, its RMSE remains smaller than those of other algorithms across the entire SNR range, reflecting its advantageous performance.

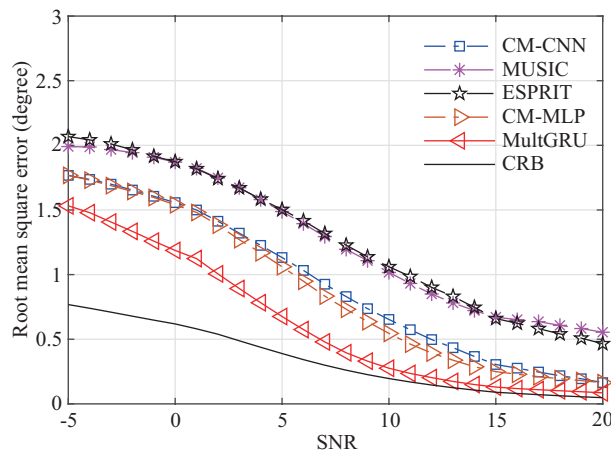


Figure 7. Analysis of the generalization ability

The training process of the MultGRU adopts an SNR range of $[0 \text{ dB} : 1 \text{ dB} : 15 \text{ dB}]$, while subsequent simulation experiments extend the SNR range to $[-5 \text{ dB} : 1 \text{ dB} : 20 \text{ dB}]$. As shown in Figure 7, the RMSE variation trends are consistent with those in Figure 6. Notably, the MultGRU remains robust and superior to other comparative algorithms even when the SNR is below 0 dB or exceeds 15 dB. Furthermore, it can also be observed that regardless of the fixed SNR, among these algorithms, the RMSE of the MultGRU is the closest to the CRB, which also indicates that the MultGRU can achieve higher accuracy in DOA estimation.

Notably, the above experiments focus on specific SNR ranges and algorithm comparisons. In future exploration, several promising directions exist, such as investigating the generalization performance under complex scenarios (including mixed noise environments and scenarios with diverse array configurations) to more comprehensively validate the applicability of the MultGRU.

4.3 Performance under different numbers of snapshots

In practical applications, the number of snapshots directly affects the performance of DOA estimation. That is, a finite sampling length will reduce the effective information carried in the data, which will also decrease the DOA estimation accuracy. On this basis, experiments are conducted to evaluate the DOA estimation performance of these algorithms under varying numbers of snapshots, with a fixed SNR of 10 dB. As depicted in Figure 8, both the CM-CNN and the CM-MLP demonstrate improved DOA estimation accuracy as the number of snapshots increases from 100 to 1,000. Meanwhile, although the MUSIC and the ESPRIT show a trend of gradual performance enhancement as the number of snapshots grows, their relatively large RMSEs indicate lower DOA estimation accuracy compared to deep learning-based algorithms.

For the MultGRU, observable performance improvement accompanies the increase in the number of snapshots. Notably, across both low and high numbers of snapshots, it outperforms other compared algorithms in achieving the best DOA estimation accuracy. Additionally, Figure 8 reveals that deep learning-based DOA estimation algorithms possess distinct advantages over the model-based algorithms under the same number of snapshots, a feature of particular significance for resource-constrained application scenarios.

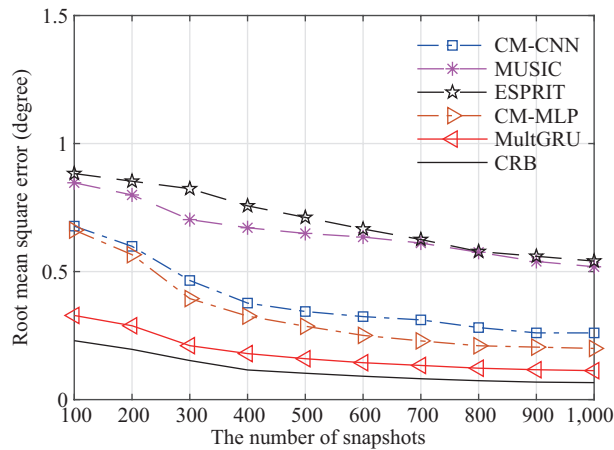


Figure 8. Performance comparison of various algorithms as a function of the number of snapshots

These results demonstrate that increasing the number of snapshots has a positive impact on the performance of DOA estimation algorithms. Therefore, modulating the number of snapshots based on specific application requirements tends to contribute to enhancing the performance of DOA estimation systems. The performance advantage of the MultGRU also lies in the fact that both level networks of the MultGRU directly establish a mapping relationship between the covariance matrix of the array output signals and the directions of the incident sources. Although a small number of snapshots can lead to a relatively large estimation deviation of the covariance matrix, as long as the training data includes such a scenario, the MultGRU can also establish an accurate mapping relationship through learning. Therefore, it has good adaptability to the estimation errors of the covariance matrix.

4.4 Performance under different numbers of sensors

Theoretical analysis elucidates that the number of sensors within a UCA exerts a substantial influence on the DOA estimation accuracy. Specifically, as the number of sensors in the array increases, the performance of DOA estimation will see a corresponding improvement.

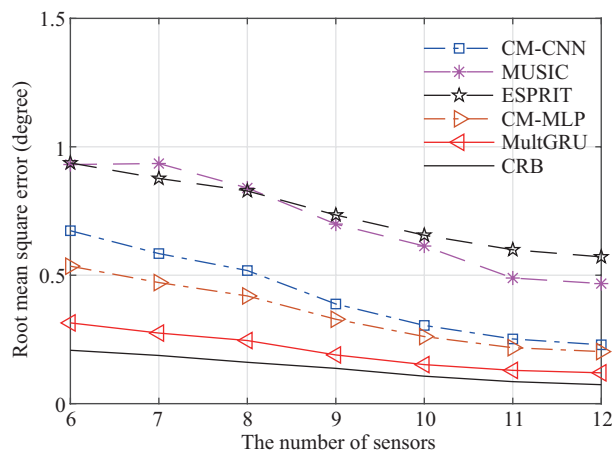


Figure 9. Performance comparison of various algorithms as a function of the number of sensors

To verify the impact of the number of sensors in a UCA on the DOA estimation accuracy and robustness of the MultGRU, simulations are conducted under an SNR of 10 dB and a number of snapshots of 300. by increasing the

number of sensors from 6 to 12. As shown in Figure 9, results indicate that with the increase in the number of sensors, the RMSEs of all the compared algorithms exhibit a decreasing trend, which is consistent with the theoretical understanding that more sensors enhance DOA estimation accuracy.

Among these algorithms, the MultGRU consistently yields the lowest RMSE across all tested numbers of sensors, showcasing its superior performance. For model-based algorithms like the MUSIC and the ESPRIT, their DOA estimation performance improvement is less evident with fewer numbers of sensors. Although their performance improves significantly as the number of sensors grows, it still lags behind deep learning-based algorithms such as the CM-CNN and the CM-MLP.

Table 3. Comprehensive performance analysis of different algorithms

Scenario	Algorithm	Average RMSE (degrees)	Relative improvement rate over MUSIC	Relative improvement rate over CM-MLP
SNR (0-15 dB)	MUSIC	1.1200	0%	-
	ESPRIT	1.2154	-	-
	CM-CNN	0.8184	26.93%	0.06%
	CM-MLP	0.8189	26.88%	0%
	MultGRU	0.5231	53.29%	36.10%
SNR (-5-20 dB)	MUSIC	1.2681	0%	-
	ESPRIT	1.2768	-	-
	CM-CNN	0.9256	27.01%	-
	CM-MLP	0.8744	31.05%	0%
	MultGRU	0.6205	51.07%	29.04%
Number of snapshots (100-1,000)	MUSIC	0.6549	0%	-
	ESPRIT	0.6998	-	-
	CM-CNN	0.3900	40.45%	-
	CM-MLP	0.3330	49.15%	0%
	MultGRU	0.1797	72.56%	46.04%
Number of sensors (6-12)	MUSIC	0.7107	0%	-
	ESPRIT	0.7433	-	-
	CM-CNN	0.4213	40.72%	-
	CM-MLP	0.3480	51.03%	0%
	MultGRU	0.2037	71.34%	41.47%

Further analysis reveals that as the number of sensors increases, the MultGRU maintains a relatively stable performance trend. Compared with the other algorithms, the RMSE variation of the MultGRU is smaller, reflecting its better robustness in DOA estimation.

As shown in Table 3, the MultGRU demonstrates remarkable advantages across various scenarios. Under different SNR scenarios, its average RMSE is far lower than that of algorithms like the MUSIC and the ESPRIT. The relative improvement rate over the MUSIC exceeds 50%, and there is also a considerable enhancement compared to the deep learning-based CM-MLP. When facing variations in the number of snapshots and sensors, the RMSE of the MultGRU remains at a low level, with the relative improvement rate reaching as high as 70% over the MUSIC. Compared with the CM-MLP, the improvement rate of the MultGRU in terms of RMSE remains above 40%. It can be seen that whether resisting noise interference, adapting to fluctuations in the number of snapshots, or matching different sensor configurations, the MultGRU, with lower errors and a higher improvement rate, comprehensively exhibits accurate and stable performance in DOA estimation tasks, significantly outperforming other algorithms.

4.5 Performance analysis for two sources

To further analyze the accuracy and resolution of the MultGRU, this section considers the scenario where two sources are incident. During the network training process, while ensuring that other parameters remain unchanged, the number of incident sources is randomly selected within the range of 1 to 4, and for each case, the angles of the incident sources are randomly generated within the range of 0° to 90° . Relying on these settings, a training set is generated to train the MultGRU.

We evaluate the separation ability of two sources through the probability of resolution [30]. The two sources are considered to be resolvable if the following criterion can be satisfied:

$$\Delta(\theta_1, \theta_2) = f(\theta_m) - \frac{1}{2} [f(\theta_1) + f(\theta_2)] > 0 \quad (14)$$

In Equation (14), θ_1 and θ_2 are two signal arrival angles, θ_m is the mean of θ_1 and θ_2 , and $f(\cdot)$ is the reciprocal of the spatial spectrum.

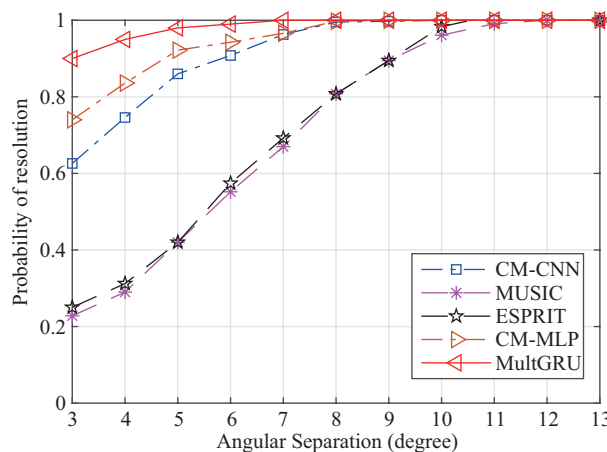


Figure 10. DOA estimation for two sources: probability of resolution

Figure 10 shows the probability of resolution for these algorithms for angular separations in the range of 3° to 13° between two incident sources. It can be seen that the probability of resolution of the subspace-based MUSIC and ESPRIT is significantly lower than that of the deep learning-based CM-CNN and CM-MLP at small angular separations, and only gradually increases to a stable state as the angular separation increases. For deep learning-based algorithms, when the angular separation of incident sources is small, the CM-CNN exhibits a lower probability of resolution compared to the CM-MLP. However, when the angular separation exceeds 8° , both algorithms can completely resolve two incident sources. This indicates that the CM-MLP has a higher resolution when the incident sources are close to each other.

Considering the MultGRU, the probability of resolution reaches over 0.9 even at an angular separation of 3° . As the angular separation increases, the probability of resolution quickly reaches 1, meaning it can completely resolve the two incident sources and maintains the highest stability throughout the process.

5. Field-deployed scenario experiments

To further ascertain the efficacy of the MultGRU, field-deployed scenario experiments are conducted, which are shown in Figure 11. That is, experiments are conducted in an urban environment with interference from high-rise buildings,

vehicles, and electronic devices. A UCA is formed by connecting 5 omnidirectional antennas to a KrakenSDR receiver. A small UAV equipped with a signal source serves as the target source, and experiments are conducted on the GNU Radio platform. To safeguard the precision of DOA estimation, antenna and phase corrections are conducted. During the experiments, the UAV rotates in 1° increments, and signals are collected once via the KrakenSDR. The signal source covers an angular range from 0° to 90° . Each collected signal is divided into some segments with 500 snapshots, and the corresponding DOA is labeled for each segment. The dataset is partitioned into training (80%) and test (20%) sets for developing and evaluating the MultGRU.



Figure 11. Signal acquisition system

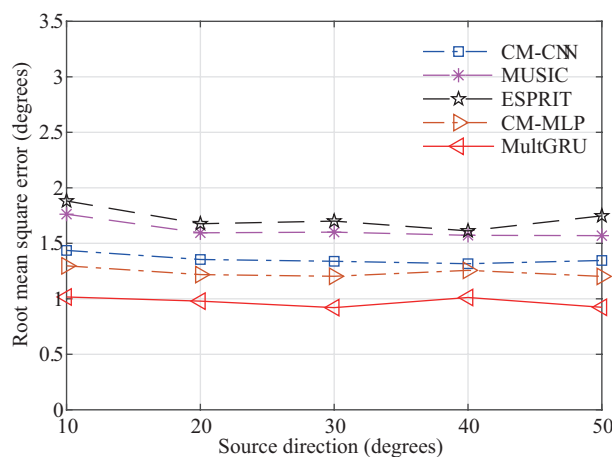


Figure 12. DOA estimation performance of different algorithms

According to the experimental results in Figure 12, it is evident that in real low-altitude complex electromagnetic environments, the performance comparison of each algorithm is consistent with that in the simulation experiments. The RMSEs that vary across various signal source incident angles of the deep learning-based DOA estimation algorithms (CM-CNN and CM-MLP) are significantly lower than those of traditional DOA estimation algorithms (ESPRIT and MUSIC), with the MultGRU achieving the smallest RMSE. The results indicate that the MultGRU consistently surpasses its counterparts when applied to real-world data, highlighting its practical robustness.

6. Computational complexity analysis

The computational complexity of different DOA estimation algorithms is evaluated using a Mac mini M4 in MATLAB. To benchmark performance, each algorithm (ESPRIT, MUSIC, CM-CNN, CM-MLP, and MultGRU) is run for 1,900 independent trials. Their respective average runtimes are 22.8835s, 26.7828s, 29.5039s, 27.4818s, and 22.5183s.

The findings indicate that among subspace-based DOA estimation algorithms, the ESPRIT, which avoids the spectral peak search, has lower computational complexity than that of the MUSIC. The computational complexities of the CM-CNN and the CM-MLP are slightly higher than those of typical subspace-based DOA estimation algorithms. However, the computational complexity of the MultGRU is slightly lower than that of the ESPRIT, rendering the MultGRU the most efficient among these algorithms.

7. Conclusions

To tackle the challenges where traditional DOA estimation algorithms depend on a priori information about signals and arrays (along with model mismatch), this work proposes a novel DOA estimation algorithm termed MultGRU, which is based on deep learning networks. The MultGRU autonomously captures the inherent characteristics of the array output signals and the intricate interactions between signals and noise. By designing a GRU network to roughly classify the DOA interval, and further refining the DOA using multiple parallel subGRU networks, the MultGRU eliminates the manual feature and model design process required by traditional algorithms, improves the performance and reliability of DOA estimation, and can adapt to more application scenarios. Simulation experiments demonstrate that, compared with other algorithms, the MultGRU delivers superior DOA estimation efficiency, particularly in terms of precision and resilience across diverse scenarios. These findings also highlight the potential of deep learning to be applied to DOA estimation.

Acknowledgement

This work was supported in part by the Zhejiang Province College Students' Innovation and Entrepreneurship Training Program Project under Grant: s202510350029, and the Zhejiang Province College Students' Science and Technology Innovation Activity Plan (New Seedling Talent Plan) under Grant: 2025R451A006.

Conflict of interest

The authors declare no competing financial interest.

References

- [1] Ma J, Ma H, Liu H, Liu W, Cheng X. A novel DOA estimation for low-elevation target method based on multiscattering center equivalent model. *IEEE Geoscience and Remote Sensing Letters*. 2023; 20: 1-5. Available from: <https://doi.org/10.1109/LGRS.2023.3242977>.
- [2] Xu F, Zheng H, Vorobyov SA. Tensor-based 2-D DOA estimation for L-shaped nested array. *IEEE Transactions on Aerospace and Electronic Systems*. 2024; 60(1): 604-618. Available from: <https://doi.org/10.1109/TAES.2023.3326793>.
- [3] Zhong X, Premkumar AB, Madhukumar AS. Particle filtering for acoustic source tracking in impulsive noise with alpha-stable process. *IEEE Sensors Journal*. 2013; 13(2): 589-600. Available from: <https://doi.org/10.1109/JSEN.2012.2223209>.
- [4] Cong J, Wang X, Lan X, Liu W. A generalized noise reconstruction approach for robust DOA estimation. *IEEE Transactions on Radar Systems*. 2023; 1: 382-394. Available from: <https://doi.org/10.1109/TRS.2023.3299184>.

- [5] Ashok C, Venkateswaran N. Manifold ambiguity-free low complexity DOA estimation method for unfolded co-prime arrays. *IEEE Communications Letters*. 2021; 25(6): 1886-1890. Available from: <https://doi.org/10.1109/LCOMM.2021.3059673>.
- [6] Schmidt R. Multiple emitter location and signal parameter estimation. *IEEE Transactions on Antennas and Propagation*. 1986; 34(3): 276-280. Available from: <https://doi.org/10.1109/TAP.1986.1143830>.
- [7] Liu Z, Wu J, Yang S, Lu W. DOA estimation method based on EMD and MUSIC for mutual interference in FMCW automotive radars. *IEEE Geoscience and Remote Sensing Letters*. 2022; 19: 1-5. Available from: <https://doi.org/10.1109/LGRS.2021.3058729>.
- [8] Li J, Li D, Li X. A real-valued Toeplitz matrix method for DOA estimation. *Canadian Journal of Electrical and Computer Engineering*. 2020; 43(4): 350-356. Available from: <https://doi.org/10.1109/CJECE.2020.3005226>.
- [9] Wang G, Kang Y, Wang H. Low-complexity DOA estimation algorithm based on real-valued sparse Bayesian learning. *Circuits, Systems, and Signal Processing*. 2024; 43: 4319-4338. Available from: <https://doi.org/10.1007/s00034-024-02649-7>.
- [10] Dong X, Zhao J, Sun M, Zhang X. Non-circular signal DOA estimation with nested array via off-grid sparse Bayesian learning. *Sensors*. 2023; 23(21): 8907. Available from: <https://doi.org/10.3390/s23218907>.
- [11] Zhang J, Chu P, Liao B. DOA estimation in impulsive noise based on FISTA algorithm. *Remote Sensing*. 2023; 15(3): 565. Available from: <https://doi.org/10.3390/rs15030565>.
- [12] He H, Wen CK, Jin S, Li GY. Deep learning-based channel estimation for beamspace mmWave massive MIMO systems. *IEEE Wireless Communications Letters*. 2018; 7(5): 852-855. Available from: <https://doi.org/10.1109/LWC.2018.2832128>.
- [13] Ge S, Li K, Rum SNBM. Deep learning approach in DOA estimation: A systematic literature review. *Mobile Information Systems*. 2021; 2021: 6392875. Available from: <https://doi.org/10.1155/2021/6392875>.
- [14] Xu X, Huang Q. MD-DOA: A model-based deep learning DOA estimation architecture. *IEEE Sensors Journal*. 2024; 24(12): 20240-20253. Available from: <https://doi.org/10.1109/JSEN.2024.3396337>.
- [15] Huang H, Yang J, Huang H, Song Y, Gui G. Deep learning for super-resolution channel estimation and DOA estimation based massive MIMO system. *IEEE Transactions on Vehicular Technology*. 2018; 67(9): 8549-8560. Available from: <https://doi.org/10.1109/TVT.2018.2851783>.
- [16] Yu J, Wang Y. Deep learning-based multipath DoAs estimation method for mmWave massive MIMO systems in low SNR. *IEEE Transactions on Vehicular Technology*. 2023; 72(6): 7480-7490. Available from: <https://doi.org/10.1109/TVT.2023.3239402>.
- [17] Wang W, Zhou L, Ye K, Sun H, Hong S. A DOA estimation method based on an improved transformer model for uniform linear arrays with low SNR. *IET Signal Processing*. 2024; 2024: 6666395. Available from: <https://doi.org/10.1049/2024/6666395>.
- [18] Ji J, Mao W, Xi F, Chen S. TransMUSIC: A transformer-aided subspace method for DOA estimation with low-resolution ADCS. In: *IEEE International Conference on Acoustics, Speech and Signal Processing (ICASSP)*. Seoul, Korea: IEEE; 2024. p.8576-8580.
- [19] Zhao X, Atli Benediktsson J, Yang Y, Chen KS, Örn Úlfarsson M. Exploring transformer-based direction-of-arrival estimation over sea surface: A BERT approach with physics-based loss function. *IEEE Transactions on Geoscience and Remote Sensing*. 2024; 62: 1-13. Available from: <https://doi.org/10.1109/TGRS.2024.3440224>.
- [20] Hu W, Wang Q. DOA estimation for UCA in the presence of mutual coupling via error model equivalence. *IEEE Wireless Communications Letters*. 2020; 9(1): 121-124. Available from: <https://doi.org/10.1109/LWC.2019.2944816>.
- [21] Sarker IH. Deep learning: A comprehensive overview on techniques, taxonomy, applications and research directions. *SN Computer Science*. 2021; 2: 420. Available from: <https://doi.org/10.1007/s42979-021-00815-1>.
- [22] Yu D, Deng L. Deep learning and its applications to signal and information processing [Exploratory DSP]. *IEEE Signal Processing Magazine*. 2011; 28(1): 145-154. Available from: <https://doi.org/10.1109/MSP.2010.939038>.
- [23] Cao Z, Li D. Beamforming and lightweight GRU neural network combination model for multi-channel speech enhancement. *Signal, Image and Video Processing*. 2024; 18: 5677-5683. Available from: <https://doi.org/10.1007/s11760-024-03263-5>.
- [24] Liu ZM, Zhang C, Yu PS. Direction-of-arrival estimation based on deep neural networks with robustness to array imperfections. *IEEE Transactions on Antennas and Propagation*. 2018; 66(12): 7315-7327. Available from: <https://doi.org/10.1109/TAP.2018.2874430>.

- [25] Papageorgiou GK, Sellathurai M, Eldar YC. Deep networks for direction-of-arrival estimation in low SNR. *IEEE Transactions on Signal Processing*. 2021; 69: 3714-3729. Available from: <https://doi.org/10.1109/TSP.2021.3089927>.
- [26] Roy R, Kailath T. ESPRIT-estimation of signal parameters via rotational invariance techniques. *IEEE Transactions on Acoustics, Speech, and Signal Processing*. 1989; 37(7): 984-995. Available from: <https://doi.org/10.1109/29.32276>.
- [27] Liang Y, Cui W, Shen Q, Liu W, Wu H. Cramér-Rao bound for DOA estimation exploiting multiple frequency pairs. *IEEE Signal Processing Letters*. 2021; 28: 1210-1214. Available from: <https://doi.org/10.1109/LSP.2021.3088051>.
- [28] Liu TH, Mendel JM. A subspace-based direction finding algorithm using fractional lower order statistics. *IEEE Transactions on Signal Processing*. 2001; 49(8): 1605-1613. Available from: <https://doi.org/10.1109/78.934131>.
- [29] Qu X, Xie L, Tan W. Iterative constrained weighted least squares source localization using TDOA and FDOA measurements. *IEEE Transactions on Signal Processing*. 2017; 65(15): 3990-4003. Available from: <https://doi.org/10.1109/TSP.2017.2703667>.
- [30] Zhang QT. Probability of resolution of the MUSIC algorithm. *IEEE Transactions on Signal Processing*. 1995; 43(4): 978-987. Available from: <https://doi.org/10.1109/78.376849>.